Form factors and branching ratios of the FCNC $B \to a_1 \ell^+ \ell^-$ decays

R. Khosravi *

Department of Physics, Isfahan University of Technology, Isfahan 84156-83111, Iran

Abstract

We analyze the semileptonic $B \to a_1 \ell^+ \ell^-$, $\ell = \tau, \mu, e$ transitions in the frame work of the three-point QCD sum rules in the standard model. These rare decays governed by flavor-changing neutral current transition of $b \to d$. Considering the quark condensate contributions, the relevant form factors as well as the branching fractions of these transitions are calculated.

PACS numbers: 11.55.Hx, 13.20.He, 14.40.Be

* e-mail: rezakhosravi @ cc.iut.ac.ir

I. INTRODUCTION

The decays governed by flavor-changing neutral current (FCNC) transitions are very sensitive to the gauge structure of the standard model (SM) which provide an excellent way to test such a model. These decays, prohibited at the tree-level, take place at loop level by electroweak penguin and weak box diagrams. The FCNC transitions can be suppressed due to their proportionality to the small Cabibbo-Kobayashi-Maskawa matrix elements (for instance see [1]). Among these, the FCNC semileptonic decays of the B meson occupy a special place in both experimental measurements and theoretical studies for the precision test of the SM due to more simplicity.

So far, the form factors of the semileptonic decay $B \to a_1 \ell \nu$ have been studied via the different approaches such as the covariant light front quark model (LFQM) [2], the constituent quark-meson model (CQM) [3], the light cone QCD sum rules (LCSR) [4], and the QCD sum rules (SR) [5]. However, the obtained results of these methods are different from each other.

In this work, we calculate the transition form factors of the FCNC semileptonic decays $B \to a_1(1260)\ell^+\ell^-/\nu\bar{\nu}$ in the framework of the three-point QCD sum rules method (3PSR). Considering the transition form factors for such decays in the framework of different theoretical methods has two-fold importance:

1) A number of the physical observables such as branching ratio, the forward-backward asymmetry and lepton polarization asymmetry, which have important roles in testing the SM and searching for new physics beyond the SM, could be investigated.

2) These form factors can be also used to determine the factorization of amplitudes in the non-leptonic two-body decays.

On the other hand, any experimental measurements of the present quantities and a comparison with the theoretical predictions can give valuable information about the FCNC transitions and strong interactions in $B \to a_1\ell^+\ell^-/\nu\bar{\nu}$ decays.

The plan of the present paper is as follows: In Sec. II, we describe the sum rules method to calculate the form factors of the FCNC $B \to a_1$ transition. Section III is devoted to the numerical analysis of the form factors and branching ratio values of the semileptonic $B \to a_1$ decays, with and without the long-distance (LD) effects.

II. FORM FACTORS OF THE FCNC $B \to a_1$ TRANSITION IN 3PSR

In the SM, the rare semileptonic decays which occur via $b \to d\ \ell^+\ell^-$ transition is described by the effective Hamiltonian as [6]:

$$H_{\rm eff} = -\frac{G_F}{\sqrt{2}} V_{tb} V_{td}^* \sum_{i=1}^{10} C_i(\mu) O_i(\mu)\ . \tag{1}$$

where V_{tb} and V_{td} are the elements of the CKM matrix, and $C_i(\mu)$ are the Wilson coefficients. It should be noted that the CKM-suppressed contributions proportional to $V_{ub}V_{ud}^*$ is neglected, also the approximation $|V_{tb}V_{td}^*| \simeq |V_{cb}V_{cd}^*|$ is adopted [7]. The standard set of the local operators for $b \to d\ell^+\ell^-$ transition is written as [8]:

$$\begin{array}{ll}
O_1 = (\bar{d}_i c_j)_{V-A}, (\bar{c}_j b_i)_{V-A}, & O_2 = (\bar{d}c)_{V-A}(\bar{c}b)_{V-A}, \\
O_3 = (\bar{d}b)_{V-A}\sum_q(\bar{q}q)_{V-A}, & O_4 = (\bar{d}_i b_j)_{V-A}\sum_q(\bar{q}_j q_i)_{V-A}, \\
O_5 = (\bar{d}b)_{V-A}\sum_q(\bar{q}q)_{V+A}, & O_6 = (\bar{d}_i b_j)_{V-A}\sum_q(\bar{q}_j q_i)_{V+A}, \\
O_7 = \frac{e}{8\pi^2} m_b (\bar{d}\sigma^{\mu\nu}(1+\gamma_5)b)F_{\mu\nu}, & O_8 = \frac{g}{8\pi^2} m_b(\bar{d}_i\sigma^{\mu\nu}(1+\gamma_5)T_{ij}b_j)G_{\mu\nu}, \\
O_9 = \frac{e}{8\pi^2}(\bar{d}b)_{V-A}(\bar{l}l)_V, & O_{10} = \frac{e}{8\pi^2}(\bar{d}b)_{V-A}(\bar{l}l)_A
\end{array} \tag{2}$$

where $G_{\mu\nu}$ and $F_{\mu\nu}$ are the gluon and photon field strengths, respectively; T_{ij} are the generators of the $SU(3)$ color group; i and j denote color indices. Labels $(V \pm A)$ stand for $\gamma^\mu(1 \pm \gamma^5)$. $O_{1,2}$ are current-current operators, O_{3-6} are QCD penguin operators, $O_{7,8}$ are magnetic penguin operators, and $O_{9,10}$ are semileptonic electroweak penguin operators.

The most relevant contributions to $B \to a_1\ell^+\ell^-$ transitions are given by the O_7 and $O_{9,10}$, short distance (SD) contributions, as well as the tree-level four quark operators $O_{1,2}$ which have sizeable Wilson coefficients. The current-current operators $O_{1,2}$ involves an intermediate charm-loop, LD contributions, coupled to the lepton pair via the virtual photon (see Fig. 1). This contribution has got the same form factor dependence as C_9 and can therefore be absorbed into an effective Wilson coefficient $C_9^{\rm eff}$ [9].

Therefore, the effective Hamiltonian for $B \to a_1\ell^+\ell^-$ decays which occur via $b \to d\ell^+\ell^-$ loop transition can be written as:

$$\begin{aligned}
H_{\rm eff} &= \frac{G_F\alpha}{2\sqrt{2}\pi} V_{tb}V_{td}^* \Bigg[C_9^{\rm eff}\bar{d}\gamma_\mu(1-\gamma_5)b\ \bar{l}\gamma_\mu l + C_{10}\bar{d}\gamma_\mu(1-\gamma_5)b\ \bar{l}\gamma_\mu\gamma_5 l \\
&- 2C_7^{\rm eff}\frac{m_b}{q^2}\bar{d}\ i\sigma_{\mu\nu}q^\nu(1+\gamma_5)b\ \bar{l}\gamma_\mu l\Bigg],
\end{aligned} \tag{3}$$

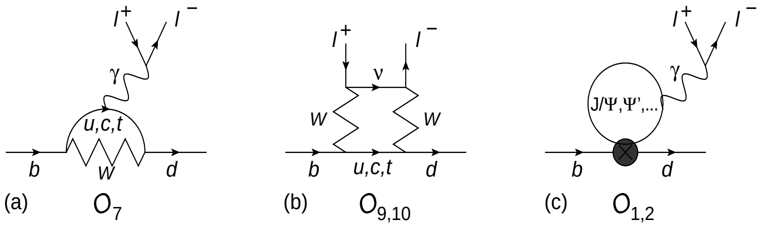

FIG. 1: (a) and (b) O_7 and $O_{9,10}$ short distance contributions. (c) $O_{1,2}$ long distance charm-loop contribution.

where $C_7^{\rm eff} = C_7 - C_5/3 - C_6$. The effective Wilson coefficients $C_9^{\rm eff}(q^2)$, are given as

$$C_9^{\rm eff}(q^2) = C_9 + Y(q^2)\,. \tag{4}$$

The function $Y(q^2)$ contains the LD contributions coming from the real $c\bar{c}$ intermediate states called charmonium resonances. Two resonances, J/ψ and ψ', are narrow and the last four resonances, $\psi(3370)$, $\psi(4040)$, $\psi(4160)$ and $\psi(4415)$, are above the $D\bar{D}$-threshold and as a consequence the width is much larger. The explicit expressions of the $Y(q^2)$ can be found in [9] (see also [8, 10]).

To calculate the form factors of the FCNC $B \to a_1$ transition, within 3PSR method, we start with the following correlation functions constructed from the transition currents $J_\mu^{V-A} = \bar{d}\gamma_\mu(1-\gamma_5)b$ and $J_\mu^T = \bar{d}\, i\sigma_{\mu\eta}q^\eta(1+\gamma_5)b$ as follows:

$$\Pi_{\mu\nu}^{V-A\ (T)}(p^2, p'^2, q^2) = \int d^4x d^4y e^{-ipx} e^{ip'y} \langle 0 \mid \mathcal{T}[J_\nu^{a_1}(y) J_\mu^{V-A\ (T)}(0) J^{B^\dagger}(x)] \mid 0\rangle\,, \tag{5}$$

where $J^B = \bar{u}\gamma_5 b$, and $J_\nu^{a_1} = \bar{u}\gamma_\nu\gamma_5 d$ are the interpolating currents of the initial and final meson states, respectively. In the QCD sum rules approach, we can obtain the correlation functions of Eq. (5) in two languages: the hadron language, which is the physical or phenomenological side, and the quark-gluon language called the QCD or theoretical side. Equating two sides and applying the double Borel transformations with respect to the momentum of the initial and final states to suppress the contribution of the higher states and continuum, we get sum rule expressions for our form factors. To drive the phenomenological part, two complete sets of intermediate states with the same quantum numbers as the currents $J_\nu^{a_1}$ and J^B are inserted in Eq. (5). As a result of this procedure,

$$\Pi_{\mu\nu}^{V-A\ (T)}(p, p') = \frac{1}{p^2 - m_B^2}\frac{1}{p'^2 - m_{a_1}^2}\langle 0|J_\nu^{a_1}|a_1\rangle\langle a_1|J_\mu^{V-A\ (T)}|B\rangle\langle B|J^{B^\dagger}|0\rangle + \text{higher states}\,, \tag{6}$$

where p and p' are the momentum of the initial and final meson states, respectively. To get the transition matrix elements of the $B \to a_1$ with various quark models, we parameterize them in terms of the relevant form factors as

$$\begin{aligned}
\langle a_1(p',\epsilon) \mid J_\mu^{V-A} \mid B(p)\rangle &= \frac{1}{m_B+m_{a_1}} \left[2\, A(q^2)\, i\varepsilon_{\mu\lambda\alpha\beta}\epsilon^{*\lambda}p^\alpha p'^\beta + V_1(q^2)(P.q)\epsilon^*_\mu \right. \\
&+ \left. V_2(q^2)\,(\epsilon^*.p)P_\mu + V_0(q^2)\,(\epsilon^*.p)q_\mu\right] , \\
\langle a_1(p',\epsilon) \mid J_\mu^{T} \mid B(p)\rangle &= 2\, T_1(q^2)\; i\varepsilon_{\mu\lambda\alpha\beta}\epsilon^{*\lambda}p^\alpha p'^\beta + T_2(q^2)(m_B^2-m_{a_1}^2)\left[\epsilon^*_\mu - \frac{1}{q^2}(\epsilon^*.q)q_\mu\right] \\
&+ T_3(q^2)\;(\epsilon^*.p)\left[P_\mu - \frac{1}{q^2}(P.p)q_\mu\right] , \qquad (7)
\end{aligned}$$

where $P=p+p'$ and $q=p-p'$. Also m_{a_1} and ϵ are the mass and the four-polarization vector of the a_1 meson. The vacuum-to-meson transition matrix elements are defined in standard way, namely

$$\langle 0|J^B|B\rangle = -if_B\frac{m_B^2}{m_b}\,, \qquad \langle 0|J_\nu^{a_1}|a_1\rangle = f_{a_1}m_{a_1}\epsilon_\nu\ . \qquad (8)$$

Using Eq. (7), and Eq. (8) in Eq. (6), and performing summation over the polarization of the a_1 meson, we obtain

$$\begin{aligned}
\Pi_{\mu\nu}^{V-A} &= \frac{f_B m_B^2}{m_b}\frac{f_{a_1}m_{a_1}}{(p^2-m_B^2)(p'^2-m_{a_1}^2)} \times \left[\frac{2A}{m_B+m_{a_1}}(q^2)\,\varepsilon_{\mu\nu\alpha\beta}p^\alpha p'^\beta - iV_1(q^2)\,(m_B-m_{a_1})\,g_{\mu\nu}\right. \\
&-i\;\left.\frac{V_2(q^2)}{m_B+m_{a_1}}\;P_\mu p_\nu - i\frac{V_0(q^2)}{m_B+m_{a_1}}\;q_\mu p_\nu\right] + \text{excited states}\,, \\
\Pi_{\mu\nu}^{T} &= \frac{f_B m_B^2}{m_b}\frac{f_{a_1}m_{a_1}}{(p^2-m_B^2)(p'^2-m_{a_1}^2)} \times \left[2\,T_1(q^2)\,\varepsilon_{\mu\nu\alpha\beta}p^\alpha p'^\beta - iT_2(q^2)\,(m_B^2-m_{a_1}^2)\,g_{\mu\nu}\right. \\
&-i\;\left.T_3(q^2)\,P_\mu p_\nu\right] + \text{excited states}\,. \qquad (9)
\end{aligned}$$

To calculate the form factors A, $V_i(i=0,1,2)$, and $T_j(j=1,2,3)$, we will choose the structures $\varepsilon_{\mu\nu\alpha\beta}p^\alpha p'^\beta$, $g_{\mu\nu}$, $P_\mu p_\nu$, $q_\mu p_\nu$, from $\Pi_{\mu\nu}^{V-A}$ and $\varepsilon_{\mu\nu\alpha\beta}p^\alpha p'^\beta$, $g_{\mu\nu}$, and $P_\mu p_\nu$ from $\Pi_{\mu\nu}^{T}$, respectively. For simplicity, the correlations are written as

$$\begin{aligned}
\Pi_{\mu\nu}^{V-A}(p^2,p'^2,q^2) &= \Pi_A^{V-A}\,\varepsilon_{\mu\nu\alpha\beta}p^\alpha p'^\beta - i\Pi_1^{V-A}\,g_{\mu\nu} - i\Pi_2^{V-A}\,P_\mu p_\nu - i\Pi_0^{V-A}\,q_\mu p_\nu + \cdots\,, \\
\Pi_{\mu\nu}^{T}(p^2,p'^2,q^2) &= \Pi_1^{T}\,\varepsilon_{\mu\nu\alpha\beta}p^\alpha p'^\beta - i\Pi_2^{T}\,g_{\mu\nu} - i\Pi_3^{T}\,P_\mu p_\nu + \cdots\,. \qquad (10)
\end{aligned}$$

Now, we consider the theoretical part of the sum rules. For this aim, each $\Pi_k^{V-A\ (T)}$ function is defined in terms of the perturbative and nonperturbative parts as

$$\Pi^{V-A\ (T)}(p^2,p'^2,q^2) = \Pi_{\rm per}^{V-A\ (T)}(p^2,p'^2,q^2) + \Pi_{\rm nonper}^{V-A\ (T)}(p^2,p'^2,q^2)\,. \qquad (11)$$

For the perturbative part, the bare-loop diagrams are considered. With the help of the double dispersion representation, the bare-loop contribution is written as

$$\Pi_{\rm per}^{V-A\ (T)} = -\frac{1}{(2\pi)^2}\int ds'\int ds\frac{\rho^{V-A\ (T)}(s,s',q^2)}{(s-p^2)(s'-p'^2)} + \text{ subtraction terms}\,,$$

where ρ is spectral density. The spectral density is obtained from the usual Feynman integral for the bare-loop by replacing $\frac{1}{p^2-m^2}\to -2\pi i\delta(p^2-m^2)$. After standard calculations for the spectral densities $\rho_k^{V-A\ (T)}$, where k is related to each structure in Eq. (10), we have

$$\begin{aligned}
\rho_A^{V-A} &= 3\,s'\,\Lambda^{-3}\,(u-2\,\Delta)\,m_b\,,\\
\rho_0^{V-A} &= -\frac{3}{2}\,s'\,\Lambda^{-5}\,\Big(12\,u\Delta\,s'-4\,ss'^2-2\,u^2s'\,-12\,s'\,\Delta^2-2\,sus'-6\,u\Delta^2-u^3+6\,u^2\Delta\Big)\,m_b\,,\\
\rho_1^{V-A} &= -\frac{3}{2}\,s'\,\Lambda^{-3}\,\left(2\,ss'-2\,\Delta^2+2\,\Delta\,u-u^2\right)\,m_b\,,\\
\rho_2^{V-A} &= -\frac{3}{2}\,s'\,\Lambda^{-5}\,\Big(12\,u\Delta\,s'-4\,ss'^2-2\,u^2s'\,-12\,s'\,\Delta^2+2\,sus'+6\,u\Delta^2+u^3-6\,u^2\Delta\Big)\,m_b\,,\\
\rho_1^{T} &= -3\,s'\,\Lambda^{-3}\,(u-2\,\Delta)\,m_b^2\,,\\
\rho_2^{T} &= \frac{3}{2}\,s'\,\Lambda^{-3}\,\left(2\,s^2s'-2\,s\Delta^2+2\,s\Delta\,u-su^2-4\,ss'\,\Delta+sus'+u\Delta^2\right)\,,\\
\rho_3^{T} &= \frac{3}{2}\,s'\,\Lambda^{-5}\,\Big(4\,s^2s'^2+2\,us^2s'+6\,sus'^2-8\,ss'^2\Delta+8\,\Delta\,uss'-4\,ss'\,\Delta^2-7\,su^2s'+su^3\\
&- 6\,su^2\Delta+6\,su\Delta^2+6\,u\Delta^2s'-4\,u^2\Delta\,s'+4\,\Delta\,u^3-5\,u^2\Delta^2\Big)\,, \qquad (12)
\end{aligned}$$

where $u=s+s'-q^2$, $\Lambda=\sqrt{u^2-4ss'}$, and $\Delta=s-m_b^2$.

Now, the nonperturbative part contributions to the correlation functions are discussed (Eq. (11)). In QCD, the three point correlation function can be evaluated by the operator product expansion (OPE) in the deep Euclidean region. Up to dimension 6, the operators are determined by the contribution of the bare-loop, and power corrections coming from dimension-3 $\langle\bar\psi\psi\rangle$, dimension-4 $\langle G^2\rangle$, dimension-5 $m_0^2\langle\bar\psi\psi\rangle$, and dimension-6 $\langle\bar\psi\psi\rangle^2$ operators [5]. The bare-loop diagrams, perturbative part of the correlation functions, are discussed before. For the nonperturbative part contributions, our calculations show that the contributions coming from $\langle G^2\rangle$ and $\langle\bar\psi\psi\rangle^2$ are very small in comparison with the contributions of dimension-3 and 5 that, their contributions can be easily ignored. We introduce the nonperturbative part contributions as

$$\Pi_{\rm nonper}^{V-A\ (T)} = \langle u\bar u\rangle C^{V-A\ (T)}\,, \qquad (13)$$

where $\langle u\bar u\rangle = -(0.240\pm0.010)^3$ GeV^3 [11]. After some straightforward calculations, the explicit expressions for $C_k^{V-A\ (T)}$, are given as

$$
\begin{aligned}
C_A^{V-A} &= \frac{1}{rr'} - m_0^2\left[\frac{1}{3r^2r'} + \frac{m_b^2-q^2}{3r^2r'^2} + \frac{m_b^2}{2r^3r'}\right], \\
C_0^{V-A} &= \frac{1}{rr'} - m_0^2\left[\frac{1}{r^2r'} + \frac{m_b^2-q^2}{3r^2r'^2} + \frac{m_b^2}{2r^3r'}\right], \\
C_1^{V-A} &= \frac{(m_b^2-q^2)}{2rr'} - m_0^2\left[-\frac{1}{6rr'} + \frac{m_b^2-q^2}{6rr'^2} + \frac{3m_b^2-4q^2}{12r^2r'} + \frac{(m_b^2-q^2)^2}{6r^2r'^2} + \frac{m_b^4-m_b^2q^2}{4r^3r'}\right], \\
C_2^{V-A} &= -\frac{1}{rr'} - m_0^2\left[\frac{1}{3r^2r'} - \frac{m_b^2-q^2}{3r^2r'^2} - \frac{m_b^2}{2r^3r'}\right], \\
C_1^T &= -\frac{m_b}{rr'} - m_0^2\left[-\frac{m_b}{2r^2r'} - \frac{m_b(m_b^2-q^2)}{3r^2r'^2} - \frac{m_b^3}{2r^3r'}\right], \\
C_2^T &= \frac{(-m_b^3+m_bq^2)}{2rr'} - m_0^2\left[-\frac{m_b}{4rr'} - \frac{m_b(m_b^2-q^2)}{6rr'^2} - \frac{m_b(4m_b^2-5q^2)}{12r^2r'} - \frac{m_b(m_b^2-q^2)^2}{6r^2r'^2}\right. \\
&\left. - \frac{m_b^5-m_b^3q^2}{4r^3r'}\right], \\
C_3^T &= \frac{m_b}{2rr'} - m_0^2\left[\frac{2m_b}{3r^2r'} + \frac{m_b(m_b^2-q^2)}{8r^2r'^2} + \frac{m_b^3}{4r^3r'}\right], \qquad (14)
\end{aligned}
$$

where $r = p^2 - m_b^2$, $r' = p'^2$, and $m_0^2 = (0.8 \pm 0.2)\mathrm{GeV}^2$ [11].

The next step is to apply the Borel transformations as

$$
B_{p^2}(M^2)\left(\frac{1}{p^2-m^2}\right)^n = \frac{(-1)^n}{\Gamma(n)}\frac{e^{-m^2/M^2}}{(M^2)^n}, \qquad (15)
$$

with respect to the $p^2(p^2 \to M_1^2)$ and $p'^2(p'^2 \to M_2^2)$ on the phenomenological as well as the perturbative and nonperturbative parts of the correlation functions and equate these two representations of the correlations. The following sum rules for the form factors are derived

$$
\begin{aligned}
A'(V_i')(q^2) &= -\frac{m_b}{f_B m_B^2 f_{a_1} m_{a_1}} e^{m_B^2/M_1^2} e^{m_{a_1}^2/M_2^2} \times \left\{ -\frac{1}{4\pi^2}\int_0^{s_0'} ds' \int_{s_L}^{s_0} ds \rho_{A(i)}^{V-A} e^{-s/M_1^2} e^{-s'/M_2^2} \right. \\
&\left. + \langle u\bar{u}\rangle \times B_{p^2}(M_1^2) B_{p'^2}(M_2^2) C_{A(i)}^{V-A} \right\}, \\
T_j'(q^2) &= -\frac{m_b}{f_B m_B^2 f_{a_1} m_{a_1}} e^{m_B^2/M_1^2} e^{m_{a_1}^2/M_2^2} \times \left\{ -\frac{1}{4\pi^2}\int_0^{s_0'} ds' \int_{s_L}^{s_0} ds \rho_j^T e^{-s/M_1^2} e^{-s'/M_2^2} \right. \\
&\left. + \langle u\bar{u}\rangle \times B_{p^2}(M_1^2) B_{p'^2}(M_2^2) C_j^T \right\}, \qquad (16)
\end{aligned}
$$

where

$$
\begin{aligned}
A'(q^2) &= \frac{2A(q^2)}{m_B + m_{a_1}}\,, & V'_0(q^2) &= \frac{V_0(q^2)}{m_B + m_{a_1}}\,, \\
V'_1(q^2) &= V_1(q^2)(m_B - m_{a_1})\,, & V'_2(q^2) &= \frac{V_2(q^2)}{m_B + m_{a_1}}\,, \\
T'_1(q^2) &= 2T_1(q^2)\,, & T'_2(q^2) &= T_2(q^2)(m_B^2 - m_{a_1}^2)\,, \\
T'_3(q^2) &= T_3(q^2)\,.
\end{aligned}
$$

s_0 and s'_0 are the continuum thresholds in the B and a_1 meson channels, respectively. s_L, the lower limit of the integration over s, is: $m_b^2 + \frac{m_b^2}{m_b^2 - q^2} s'$.

III. NUMERICAL ANALYSIS

In this section, we present our numerical analysis of the form factors A, V_i, and T_j. We choose the values of the quark, lepton, and meson masses and also the leptonic decay constants as: $m_b = 4.8$ GeV [12], $m_\mu = 0.105$ GeV, $m_\tau = 1.776$ GeV, $m_{a_1} = 1.260$ GeV, $m_B = 5.280$ GeV [13], $f_{a_1} = (238 \pm 10)$ MeV [14]. For the value of the f_B, we shall use $f_B = 140$ MeV. This value of f_B corresponds to the case where $\mathcal{O}(\alpha_s)$ corrections are not taken into account (see [15, 16]).

The sum rules for the form factors contain also four auxiliary parameters: Borel mass squares M_1^2 and M_2^2 and continuum thresholds s_0 and s'_0. These are not physical quantities, so the form factors as physical quantities should be independent of them. The continuum thresholds of B and a_1 mesons, s_0 and s'_0 respectively, are not completely arbitrary; these are in correlation with the energy of the first exited state with the same quantum numbers as the considered interpolating currents. The values of the continuum thresholds calculated from the two–point QCD sum rules are taken to be $s_0 = (35 \pm 2)$ GeV^2 [17] and $s'_0 = (2.55 \pm 0.15)$ GeV^2 [14]. We search for the intervals of the Borel mass parameters so that our results are almost insensitive to their variations. One more condition for the intervals of these parameters is the fact that the aforementioned intervals must suppress the higher states, continuum and contributions of the highest-order operators. In other words, the sum rules for the form factors must converge (for more details, see [18]). As a result, we get 8 GeV$^2 \leq M_1^2 \leq 15$ GeV^2 and 2.5 GeV$^2 \leq M_2^2 \leq 4$ GeV^2.

Equation (16) shows the q^2 dependence of the form factors in the region where the sum rule is valid. To extend these results to the full region, we look for parametrization of the form factors in such a way that in the validity region of the 3PSR, this parametrization coincides with the sum rules prediction. We use two following sufficient parametrizations of the form factors with respect to q^2 as:

$$F^{(1)}(q^2) = \frac{1}{1-(\frac{q^2}{m_B^2})} \sum_{r=0}^{2} b_r \left[z^r + (-1)^r \, \frac{r}{3} \, z^4 \right] . \tag{17}$$

where $z = \frac{\sqrt{t_+-q^2}-\sqrt{t_+-t_0}}{\sqrt{t_+-q^2}+\sqrt{t_+-t_0}}$, $t_+ = (m_B + m_{a_1})^2$ and $t_0 = (m_B + m_{a_1})(\sqrt{m_B} - \sqrt{m_{a_1}})^2$ [19], and also

$$F^{(2)}(q^2) = \frac{f(0)}{1-\alpha(\frac{q^2}{m_B^2})+\beta(\frac{q^2}{m_B^2})^2} . \tag{18}$$

We evaluated the values of the parameters b_r ($r = 1, ..., 3$) of the first and $f(0)$, α, β of the second fit function for each transition form factor of the $B \to a_1$ decay, taking $M_1^2 = 10$ GeV^2 and $M_2^2 = 3$ GeV^2. Tables I and II show the values of the b_r and $f(0)$, α, β for the form factors.

TABLE I: The values of the b_r related to $F^{(1)}(q^2)$.

Parameter	$A^{(1)}$	$V_0^{(1)}$	$V_1^{(1)}$	$V_2^{(1)}$	$T_1^{(1)}$	$T_2^{(1)}$	$T_3^{(1)}$
b_0	0.44	0.35	0.28	-0.30	-0.33	-0.21	0.33
b_1	0.80	1.77	2.80	-1.79	-0.60	-2.14	1.42
b_2	3.89	0.09	15.52	0.94	-2.90	-11.34	-0.04

TABLE II: The values of the $f(0)$, α and β connected to $F^{(2)}(q^2)$.

Parameter	$A^{(2)}$	$V_0^{(2)}$	$V_1^{(2)}$	$V_2^{(2)}$	$T_1^{(2)}$	$T_2^{(2)}$	$T_3^{(2)}$
$f(0)$	0.51	0.46	0.52	-0.41	-0.37	-0.37	0.41
α	0.58	0.37	-0.52	0.34	0.58	-0.50	0.44
β	-0.39	-0.04	0.38	0.14	-0.40	0.48	-0.10

So far, several authors have calculated the form factors of the $B \to a_1 \ell \nu$ decay via the different approaches. For a comparison, the form factor predictions of the other approaches at $q^2 = 0$ are shown in Table. III. The results of other methods have been rescaled according to the form factor definition in Eq. (7). It is useful to present the relations between our form factors (A, V_i) in Eq. (7) to those used in [2–5]. The relations read

$$\begin{aligned} A &= \frac{(m_B + m_{a_1})}{(m_B - m_{a_1})} A^{[2]} = -A^{[3]}, \qquad V_0 = -\frac{(m_B + m_{a_1})}{2m_{a_1}} V_0^{[2,3]}, \\ V_1 &= V_1^{[2]} = -\frac{(m_B + m_{a_1})}{(m_B - m_{a_1})} V_1^{[3]}, \qquad V_2 = -\frac{(m_B + m_{a_1})}{(m_B - m_{a_1})} V_2^{[2]} = V_2^{[3]}. \end{aligned}$$

Also, the relation between our form factors to those used in [4] and [5] are obtained from the above equations by replacing $A^{[3]} \to -A^{[4]}$, $V_i^{[3]} \to -V_i^{[4]}$ and, $A^{[3]} \to \kappa A^{[5]}$, $V_i^{[3]} \to \kappa V_i^{[5]}$ respectively, where $\kappa = \frac{\sqrt{2}\ m_{a_1}}{g_{a_1} f_{a_1}}$.

TABLE III: Transition form factors of the $B \to a_1 \ell \nu$ at $q^2 = 0$ in various models. The results of other methods have been rescaled according to the form factor definition in Eq. (7).

Model	$A(0)$	$V_0(0)$	$V_1(0)$	$V_2(0)$
LFQM[2]	0.67	0.34	0.37	-0.29
CQM [3]	0.23	3.11	1.32	-0.55
LCSR[4]	0.48 ± 0.09	0.77 ± 0.13	0.60 ± 0.11	-0.42 ± 0.08
SR [5]	0.55 ± 0.08	0.49 ± 0.11	0.56 ± 0.07	-0.43 ± 0.04
This Work	0.51 ± 0.11	0.46 ± 0.10	0.52 ± 0.11	-0.41 ± 0.09

The errors in Table. III are estimated by the variation of the Borel parameters M_1^2 and M_2^2, the variation of the continuum thresholds s_0 and s_0', the variation of b quark mass and leptonic decay constants f_B and f_{a_1}. The main uncertainty comes from the thresholds and the decay constants, which is about $\sim 25\%$ of the central value, while the other uncertainties are small, constituting a few percent.

The dependence of the form factors, $A^{(1)}, V_i^{(1)}$, $T_j^{(1)}(q^2)$ and $A^{(2)}, V_i^{(2)}$, $T_j^{(2)}$ on q^2 extracted from the fit functions, Eqs. (17) and (18), are given in Figs. (2) and (3), respectively.

In the standard model, the rare semileptonic $B \to a_1 \ell^+ \ell^-$ and $B \to \rho \ell^+ \ell^-$ decays are described via loop transitions, $b \to d\ \ell^+ \ell^-$ at quark-level. Both mesons a_1 and ρ have the same quark content, but different masses and parities ,i.e., ρ is a vector (1^-) and a_1 is a axial vector (1^+). We have calculated the form factor values of the $B \to \rho \ell^+ \ell^-$ at $q^2 = 0$ in the SR model shown in Table. IV. Also, this table contains the results estimated for these

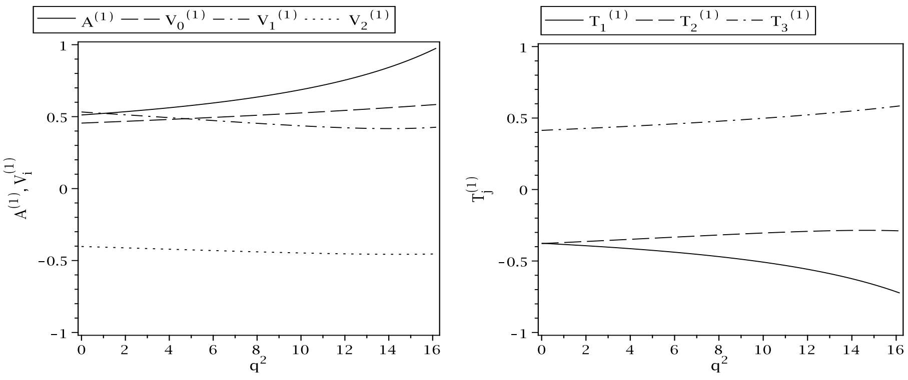

FIG. 2: The form factors $A^{(1)}, V_i^{(1)}$ and $T_j^{(1)}$ on q^2.

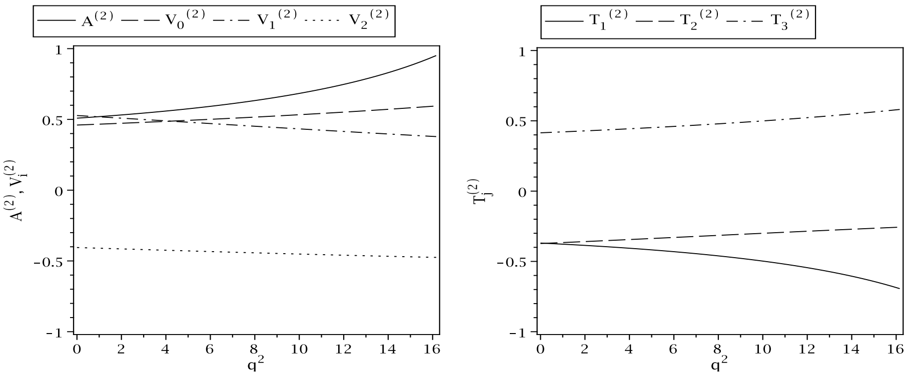

FIG. 3: The form factors $A^{(2)}, V_i^{(2)}$ and $T_j^{(2)}$ on q^2.

form factors in the frame work of the LCSR. The predicted values by us and the LSCR model are very close to each other in many cases. If a_1 behaves as the scalar partner of the ρ meson, it is expected that the $A(0)$ for the $B \to a_1$ decays is similar to the $V(0)$ for the $B \to \rho$ transitions, for example. The values obtained for $A(0)$ via two the SR and LCSR models in Table. III are larger than those for $V(0)$ in Table. IV. It appears to us that the transition form factors of the $B \to a_1$ decays are quite different of those for $B \to \rho$.

Now, we would like to evaluate the branching ratio values for the $B \to a_1 \ell^+ \ell^-$ decays.

TABLE IV: The form factor values of the $B \to \rho \ell^+ \ell^-$ at $q^2 = 0$.

Mode	$V(0)$	$A_0(0)$	$A_1(0)$	$A_2(0)$	$T_1(0)$	$T_2(0)$	$T_3(0)$
This Work	0.30 ± 0.09	0.29 ± 0.08	0.24 ± 0.06	0.20 ± 0.07	0.26 ± 0.07	0.26 ± 0.07	0.16 ± 0.05
LCSR[20]	0.32	0.30	0.24	0.22	0.27	0.27	0.18

The expressions of the differential decay width $d\Gamma/dq^2$ for the $B \to a_1 \nu\bar{\nu}$ and $B \to a_1 \ell^+\ell^-$ decays can be found in [21, 22]. These expressions contain the Wilson coefficients $C_7^{\rm eff}$, $C_9^{\rm eff}$, C_{10}, and also the CKM matrix elements V_{tb} and V_{td}. Considering $C_7^{\rm eff} = -0.313$, $C_{10} = -4.669$, $\mid V_{tb}V_{td}^* \mid = 0.008$ [8], and the form factors related to the fit functions, Eqs. (17) and (18), and after numerical analysis, the branching ratios for the $B \to a_1 \ell^+\ell^-/\nu\bar{\nu}$ are obtained as presented in Table V. In this table, we show only the values obtained considering the SD effects contributing to the Wilson coefficient $C_9^{\rm eff}$ in Eq. (4) for charged lepton case.

TABLE V: The branching ratios of the semileptonic $B \to a_1 \ell^+\ell^-$ decays, considering two groups of the form factors. 1 and 2 stand for the form factors, $F^{(1)}$ and $F^{(2)}$, respectively.

Mode	form factors	Value
$\mathrm{Br}(B \to a_1 \nu\bar{\nu}) \times 10^8$	1 2	7.41±2.44 7.78±2.32
$\mathrm{Br}(B \to a_1 e^+e^-) \times 10^8$	1 2	2.75±0.58 2.90±0.95
$\mathrm{Br}(B \to a_1 \mu^+\mu^-) \times 10^8$	1 2	2.54±0.47 2.70±0.89
$\mathrm{Br}(B \to a_1 \tau^+\tau^-) \times 10^9$	1 2	0.37±0.09 0.33±0.10

In this part, we would like to present the branching ratio values including LD effects via $C_9^{\rm eff}$. Due to in our calculations $q^2 < m^2_{\psi(4040)}$, we introduce some cuts around the narrow resonances of the J/ψ and ψ', and study the following three regions for muon:

$$\begin{aligned}
\mathrm{I}: &\qquad 2m_\mu \ \leq\ \sqrt{q^2}\ \leq\ M_{J/\psi} - 0.20\,, \\
\mathrm{II}: &\quad M_{J/\psi} + 0.04 \ \leq\ \sqrt{q^2}\ \leq\ M_{\psi'} - 0.10\,, \\
\mathrm{III}: &\quad M_{\psi'} + 0.02 \ \leq\ \sqrt{q^2}\ \leq\ m_B - m_{a_1}\,,
\end{aligned} \tag{19}$$

and the following two for tau:

$$\begin{aligned}
\mathrm{I}: &\qquad 2m_\tau \ \leq\ \sqrt{q^2}\ \leq\ M_{\psi'} - 0.02\,, \\
\mathrm{II}: &\quad M_{\psi'} + 0.02 \ \leq\ \sqrt{q^2}\ \leq\ m_B - m_{a_1}\,.
\end{aligned} \tag{20}$$

In Table VI, we present the branching ratios for muon and tau obtained using the regions shown in Eqs. (19-20), respectively. In our calculations, two groups of the form factors are considered. Here, we should also stress that the results obtained for the electron are

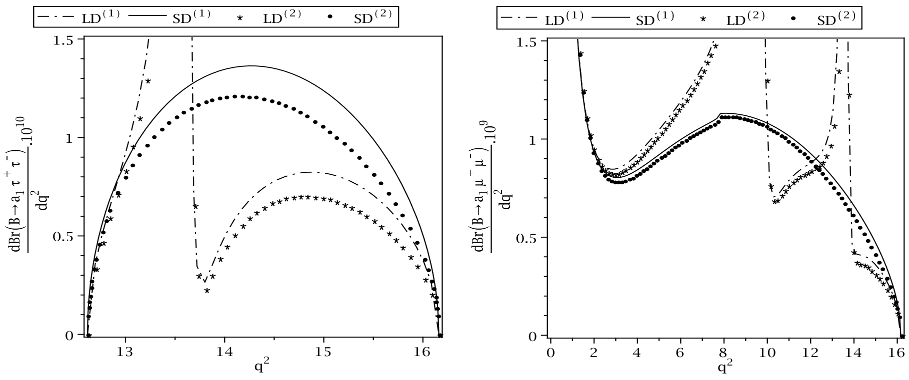

FIG. 4: The differential branching ratios of the semileptonic $B \to a_1$ decays on q^2 with and without LD effects.

very close to the results of the muon and for this reason, we only present the branching ratios for muon in our table. Considering the form factors, $F^{(1)}$ and $F^{(2)}$, the dependency

TABLE VI: The branching ratios of the semileptonic $B \to a_1\ell^+\ell^-$ decays including LD effects in three regions. 1 and 2 stand for the form factors, $F^{(1)}$ and $F^{(2)}$, respectively.

Mode	form factors	I	II	III	I+II+III
$\mathrm{Br}(B \to a_1\mu^+\mu^-) \times 10^8$	1	2.07±0.68	0.27±0.09	0.08±0.03	2.42±0.80
	2	2.30±0.76	0.26±0.09	0.07±0.03	2.63±0.88
$\mathrm{Br}(B \to a_1\tau^+\tau^-) \times 10^9$	1	undefined	0.11±0.04	0.15±0.05	0.26±0.09
	2	undefined	0.10±0.03	0.13±0.04	0.23±0.07

of the differential branching ratios on q^2 with and without LD effects for charged lepton case is shown in Fig. (4). In this figure, the solid and dash-dotted lines show the results without and with the LD effects, respectively, using the form factors, $F^{(1)}$. Also the circles and stars are the same as those lines but considering $F^{(2)}$. In Ref. [9], the interference pattern of the charm-resonances $J/\psi(3370, 4040, 4160, 4415)$ with the electroweak penguin operator O_9 in the branching fraction of $B^+ \to K^+\mu^+\mu^-$ has been investigated (in this case $q^2 \simeq 22$ GeV^2). For this purpose, the charm vacuum polarisation via a standard dispersion relation from BESII-data on $e^+e^- \to$ hadrons is extracted. In the factorisation approximation the vacuum polarisation describes the interference fully non-perturbatively. The observed interference pattern by the LHCb collaboration is opposite in sign and significantly enhanced as compared to factorisation approximation. A change of the factorisation approximation result by a factor of -2.5, which correspond to a 350%-corrections, results

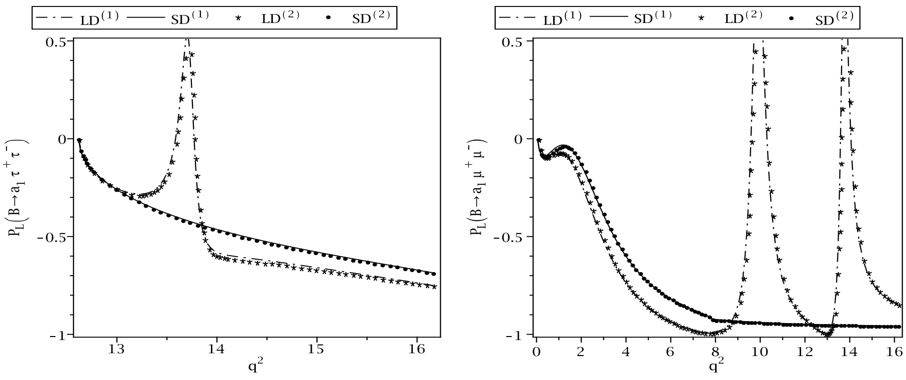

FIG. 5: The dependence of the longitudinal lepton polarization asymmetry on q^2 with and without the LD effects.

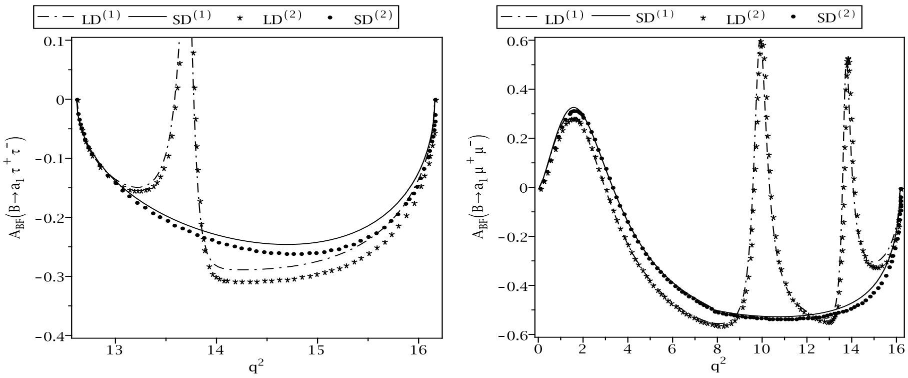

FIG. 6: The dependence of the forward-backward asymmetry on q^2 with and without the LD effects.

in a reasonable agreement with the data.

Finally, we want to calculate the longitudinal lepton polarization asymmetry and the forward-backward asymmetry for the considered decays. The expressions of the longitudinal lepton polarization asymmetry and the forward-backward asymmetry, P_L and A_{FB}, are given in [21, 22]:

The dependence of the longitudinal lepton polarization and the forward-backward asymmetries for the $B \to a_1 \ell^+ \ell^-$ decays on the transferred momentum square q^2 with and without LD effects are plotted in Figs. (5) and (6), respectively.

The measurement of these quantities in the FCNC transitions are difficult. Among the large set of inclusive and exclusive FCNC modes, a considerable attention has been put into $B \to K^* \mu^+ \mu^-$such as: measurement of the differential branching fraction and forward-backward asymmetry for $B \to K^* \ell^+ \ell^-$ [23], measurements of the angular distributions in the decays $B \to K^* \mu^+ \mu^-$ [24], differential branching fraction and angular analysis of the decay $B \to K^* \mu^+ \mu^-$ [25], Also angular distributions in the decay $B \to K^* \ell^+ \ell^-$ [26, 27]. In Ref. [27], measurements of the BABAR are presented for the FCNC decayes, $B \to K^* \ell^+ \ell^-$ including branching fractions, isospin asymmetries, direct CP violation, and lepton flavor universality for dilepton masses below and above the J/ψ resonance. Furthermore, BABAR results from an angular analysis in $B \to K^* \ell^+ \ell^-$ are reported in which both the K^* longitudinal polarization and the lepton forward-backward asymmetry are measured for dilepton masses below and above the J/ψ resonance.

In summary, the transition form factors of the semileptonic $B \to a_1 \ell^+ \ell^- / \nu \bar{\nu}$ decays were investigated in the 3PSR approach. Considering both the SD and LD effects contributing to the Wilson coefficient $C_9^{\rm eff}$ for charged lepton case, we estimated the branching ratio values for these decays. Also, for a better analysis, the dependence of the longitudinal lepton polarization and forward-backward asymmetries of these decays on q^2 were plotted.

Acknowledgments

I would like to thank M. Haghighat for his useful discussions. Partial support of the Isfahan University of Technology research council is appreciated.

[1] A. Deandrea and A. D. Polosa, Phys. Rev. **D 64**, 074012 (2001).

[2] H. Y. Cheng, C. K. Chua, and C. W. Hwang, Phys. Rev. **D 69**, 074025 (2004).

[3] A. Deandrea, R. Gatto, G. Nardulli, and A. D. Polosa, Phys. Rev. **D 59**, 074012 (1999).

[4] K. C. Yang, Phys. Rev. **D 78**, 034018 (2008).

[5] T. M. Aliev and M. Savci, Phys. Lett. **B 456**, 256 (1999).

[6] A. Khodjamirian, T. Mannel, A. A. Pivovarov, and Y. M. Wang, JHEP. **1009**, 089 (2010).

[7] J. Charles et al.(CKMfitter Group), Eur. Phys. J. **C 41**, 1 (2005).

[8] A. Faessler, Th. Gutsche, M. A. Ivanov, J. G. Korner, and V. E. Lyubovitskij, Eur. Phys. J. **C 4**, 18 (2002).

[9] J. Lyon and R. Zwicky, arXiv:1406.0566 [hep-ph].

[10] A. J. Buras and M. Muenz, Phys. Rev. **D 52**, 186 (1995).

[11] P. Colangelo and A. Khodjamirian, in *At the Frontier of Particle Physics/Handbook of QCD*, edited by M. Shifman (World Scientific, Singapore, 2001), Vol. III, p. 1495.

[12] K. C. Bowler et al. (UKQCD Collaboration), Phys. Rev. **D 52**, 5067 (1995).

[13] J. Beringer et al. (Particle Data Group), Phys. Rev. **D 86**, 010001 (2012).

[14] K. C. Yang, Nucl. Phys. **B 776**, 187 (2007).

[15] T. M. Aliev and V. L. Eletsky, Sov. J. Nucl. Phys. **38**, 936 (1983).

[16] V. M. Belyaev, V. M. Braun, A. Khodjamirian, and R. Rückl, Phys. Rev. **D 51**, 6177 (1995).

[17] M. A. Shifman, A. I. Vainshtein, and V. I. Zakharov, Nucl. Phys. **B 147**, 385 (1979).

[18] P. Colangelo and A. Khodjamirian, arXiv: 0010175 [hep-ph].

[19] C. Bourrely, I. Caprini, and L. Lellouch, Phys. Rev. **D 79**, 013008 (2009).

[20] P. Ball and R. Zwicky, Phys. Rev. **D 71**, 014029 (2005).

[21] C. Q. Geng and C. C. Liu, J. Phys. **G 29**, 1103 (2003).

[22] R. Khosravi and F. Falahati, Phys. Rev. **D 88**, 056002 (2013).

[23] J. T. Wei et al. (Belle collaboration), Phys. Rev. Lett. **103**, 171801 (2009).

[24] T. Aaltonen et al. (CDF collaboration), Phys. Rev. Lett. **108**, 081807 (2012).

[25] R. Aaij et al. (LHCb collaboration), JHEP. **1308**, 131 (2013).

[26] B. Aubert et al. (BaBar collaboration), Phys. Rev. **D 79**, 031102 (2009).

[27] G. Eigen (FPCP08 conference), arXiv:0807.4076 [hep-ex].